JCTC Journal of Chemical Theory and Computation

Article

pubs.acs.org/JCTC

Role of Electron Correlation along the Water Splitting Reaction

Shibing Chu,[†] Emanuele Coccia,[†,‡] Matteo Barborini,[¶] and Leonardo Guidoni*[,†]

[†]Dipartimento di Scienze Fisiche e Chimiche, Università degli studi dell'Aquila, Via Vetoio (Coppito), 67100 L'Aquila, Italy

[‡]Sorbonne Universités, UPMC Univ Paris 06, CNRS, Laboratoire de Chimie Théorique, CC 137-4 place Jussieu, F. 75252 Paris Cedex 05, France

[¶]CNR-NANO, Via Campi 213/a, 41125 Modena, Italy

Supporting Information

ABSTRACT: Electron correlation plays a crucial role in the energetics of reactions catalyzed by transition metal complexes, such as water splitting. In the present work we exploit the performance of various methods to describe the thermodynamics of a simple but representative model of water splitting reaction, based on a single cobalt ion as catalyst. Density Functional Theory (DFT) calculations show a significant dependence on the adopted functional, and not negligible differences with respect to CCSD(T) findings are found along the reaction cycle. We performed quantum Monte Carlo calculations using an unrestricted single Slater determinant wave function multiplied by a Jastrow factor using both DFT and fully optimized orbitals. Variational and Lattice Regularized Diffusion Monte Carlo results are in overall agreement with the CCSD(T) free-energy profile, even though differences in the description of the thermodynamics of the reaction cycle are found. NEVPT2 calculations reveal that the role of the static correlation of the different reaction steps is not large, and it is limited to only a few intermediate structures. Finally, the free-energy difference of the overall water splitting reaction computed at the quantum Monte Carlo level shows an excellent match with the experimental value of 4.92 eV, underlining the capability of these techniques to properly describe the dynamical correlation of such reactions.

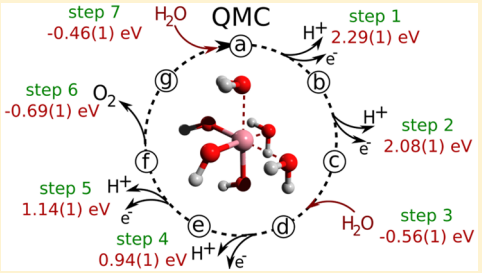

1. INTRODUCTION

Water splitting triggered by photo- and electrochemical processes represents a promising way to convert sunlight energy or electrical energy into fuels. In recent years, artificial photosynthesis[1−12] is taking this challenge by using materials and strategies which are directly or indirectly inspired by natural photosynthesis. The main obstacle for an industrial efficient conversion of solar energy into chemical fuels within an artificial photosynthetic process is the lack of suitable and cheap materials as catalysts for water oxidation. Even though materials based on noble metals are efficiently catalyzing the water splitting process, large-scale applications necessitate catalysts based on earth-abundant transition metals, such as Mn, Fe, Co, and Ni, to guarantee availability and low prices. Since in a few years nanostructured cobalt amorphous oxides were revealed to be good candidates[1,11,13−15] due to their robustness and catalytic properties. Reduced models of the amorphous cobalt oxide nanoparticles have been designed to study the structure[16,17] and reactivity[8,18,19] of water oxidation reaction. Density functional theory (DFT) has been extensively used for the quantitative description of the chemical processes involved in the artificial catalysis, thanks to the good trade-off between accuracy and computational effort permitting the study of the electronic structure of transition metal complexes.

In order to benchmark the behavior of different DFT exchange-correlation functionals and of the Hubbard correction introduced in DFT+U approaches,[19] recent ab initio calculations at coupled cluster and Møller−Plesset perturbation level of theory have been performed on a simplified reduced model, composed of only one cobalt ion coordinating three water molecules and three OH^- groups, mimicking the Co−O bonds of larger clusters.[11,19] Despite its simplicity, the ion model is fully representative of the thermodynamics of the water oxidation mechanism.[11,19] Within this catalyst, the water splitting reaction

$$2H_2O \rightarrow 4e^- + 4H^+ + O_2 \quad (1)$$

can be decomposed into seven consecutive steps, four of which are characterized by a proton-coupled electron transfer (PCET) in which one electron and one proton are released simultaneously, as shown in Figure 1. The calculation of the free-energy reaction profile for the catalytic cycle of the smallest model (Figure 1) has been carried out following the protocol proposed by Nørskov and co-workers.[20]

In the previous work by Fabris and co-workers,[19] assuming CCSD(T) results in the complete basis set (CBS) limit as the theoretical reference, standard LDA and GGA exchange-correlation functionals have been seen to fail to correctly reproduce the reaction profile, whereas hybrid B3LYP and PBE0 functionals instead display a satisfactory agreement with the CCSD(T) predictions.[19]

Received: June 22, 2016
Published: October 17, 2016

DOI: 10.1021/acs.jctc.6b00632
J. Chem. Theory Comput. 2016, 12, 5803−5810

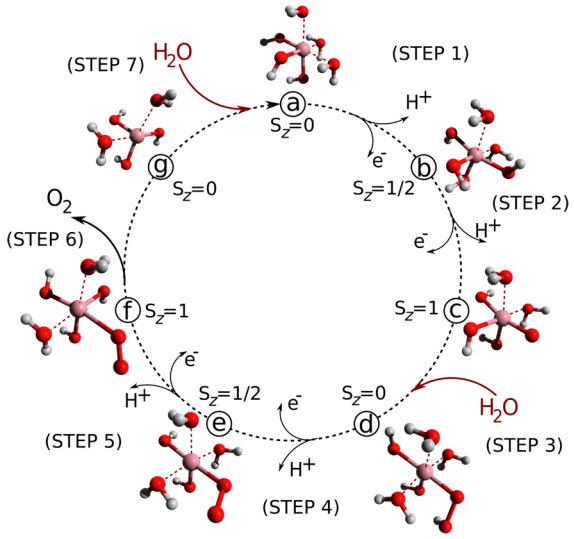

Figure 1. Reaction cycle involving the cobalt ion (in pink) model, as defined in ref 19.

To compute the free-energy profile of the reaction defined by the ion model, in the present work we consider the quantum Monte Carlo methods (QMC)[21] as a high-level alternative approach. Thanks to the embarrassing parallelism allowing one to exploit the potentiality of high-performance computing infrastructures,[22] QMC has been successfully applied to the study of the energetics and the structure of large systems with hundreds of electrons, as polyacetylene chains,[23] biochromophores[24,25] and to investigate the properties of liquid water.[26]

The wave function employed in present investigation is defined as an unrestricted single Slater determinant multiplied by a Jastrow factor. The presence of the Jastrow term, i.e. an explicit function of interparticle distances,[27] is essential to efficiently describe the high degree of dynamical correlation present in transition metal-based systems, allowing us to directly compare QMC energies with those obtained by CCSD(T). Using the B3LYP structures reported in ref 19, we have carried out variational and diffusion Monte Carlo calculations for estimating the free-energy profile of the water oxidation reaction along the ion model (Figure 1). Several functionals have been also tested against QMC and CCSD(T) results. Furthermore, we have compared the QMC results with those obtained by NEVPT2 calculations, with the aim to investigate the possible multiconfigurational nature of the cobalt-based structures along the catalytic pathway.

The work is organized as follows. In Section 2 the QMC methods and the trial wave function used are shortly introduced, together with the procedure used for computing the free-energy profile. Details on the present calculations are summarized in Section 2.3. Our results on the cobalt complex are presented and discussed in Section 3, and final comments on the use of the present QMC computational protocol for transition metal complexes as the cobalt model investigated in this work are reported in the Conclusions.

2. THEORETICAL METHODS

2.1. Quantum Monte Carlo Methods. Quantum Monte Carlo methods (QMC)[21,28] are a powerful alternative to traditional quantum chemistry and DFT methods to tackle the electronic structure calculations of atoms, molecules, and solids in which the electron correlation has a crucial role. QMC approaches are characterized by a DFT-like scalability with respect to the system size (N^d, with $3 < d < 4$ and N the number of electrons)[21,29] and by the use of algorithms that can be efficiently parallelized, making QMC calculations a competitive tool for accurate calculations on large correlated systems. Indeed, the main drawback of any QMC approach, namely the very large prefactor in the scaling preventing the systematic use of QMC in quantum chemical calculations of medium- and large-size systems, has been dramatically alleviated by the introduction of high-performance computing facilities on which QMC methods can scale up to 10^6 cores. These properties are the main reason for the growing number of QMC applications in problems of quantum chemistry and molecular physics.[27,2629–38]

Variational Monte Carlo (VMC)[39] represents the simplest method, which combines together Monte Carlo integration for computing the energy as the expectation value of the electronic Hamiltonian $\hat{H}$ and the variational principle for the ground state. The VMC energy E_{VMC}[21] is defined as the minimum of the expectation value of $\hat{H}$ over the set of parameters $\mathbf{p}$ of a trial wave function Ψ_T for a given nuclear configuration $\mathbf{R}$

$$E_{\mathrm{VMC}} = \min_{\mathbf{p}} E[\Psi_T(\mathbf{p}, \mathbf{x}, \mathbf{R})] \tag{2}$$

where (the dependence of Ψ_T with respect to $\mathbf{p}$ and $\mathbf{R}$ is here omitted)

$$E[\Psi_T] = \langle \hat{H} \rangle_{\Psi_T^2} = \frac{\int \Psi_T(\mathbf{x}) \hat{H} \Psi_T(\mathbf{x}) d\mathbf{x}}{\int \Psi_T^2(\mathbf{x}) d\mathbf{x}} \tag{3}$$

The VMC integral is written in terms of the *local energy*, $E_{\mathrm{L}} = H\hat{\Psi}_T/\Psi_T$, and of the probability density $\frac{\Psi_T^2}{\int \Psi_T^2}$

$$E[\Psi_T] = \frac{\int \Psi_T^2(\mathbf{x}) E_L(\mathbf{x}) d\mathbf{x}}{\int \Psi_T^2(\mathbf{x}) d\mathbf{x}} \tag{4}$$

and estimated as a sum over a set of spin and Cartesian coordinates $\mathbf{x}$, randomly generated according to the probability distribution $\frac{\Psi_T^2}{\int \Psi_T^2} d\mathbf{x}$.

Beyond VMC, the diffusion Monte Carlo (DMC) technique[40] is one of the most used Green's function Monte Carlo approaches, allowing one to extract the ground-state energy, within the fixed-node approximation,[40] i.e. the lowest energy associated with the nodal surface of the trial wave function. The Green's function Monte Carlo method adopted in this work is the Lattice Regularized DMC (LRDMC),[41,42] which has been demonstrated to be efficient for systems with a large number of electrons[42] and preserves the variational principle even when used in combination with nonlocal pseudopotentials.[42]

2.2. Trial Wave Function. In QMC the trial wave function Ψ is usually defined as a product of a Fermionic term $\mathcal{D}$, which provides the nodal structure, and a bosonic one, named the Jastrow factor $\mathcal{J}$, explicitly describing the interparticle correlation:[21,27]

$$\Psi(\mathbf{x}) = \mathcal{D}(\mathbf{x}) \times \mathcal{J}(\mathbf{x}) \tag{5}$$

A proper choice of the wave function ansatz guarantees an accurate description of both static and dynamical correlations, provided a full optimization of the variational parameters of the trial wave function is achieved. In our investigation the

DOI: 10.1021/acs.jctc.6b00632
J. Chem. Theory Comput. 2016, 12, 5803−5810

Fermionic part of the wave function $\mathcal{D}$ is represented by an unrestricted single Slater determinant.

The Jastrow factor is written as the exponential of a function U, $\mathcal{J} = \exp[U]$, consisting of several terms accounting for the two-body, three-body, and four-body interactions between the electrons and the nuclei[27,43,44]

$$U = U_{en} + U_{ee} + U_{een} + U_{eenn} \quad (6)$$

with the electron−nucleus U_{en}, the electron−electron U_{ee}, the electron−electron−nucleus U_{een}, and the electron−electron−nucleus−nucleus U_{eenn} contributions. The functional form of the Jastrow used in our investigation is described in refs 27 and 43. The leading contribution is the homogeneous two-electron interaction term U_{ee}, which only depends on the electron pair distance, and is used to satisfy the electron−electron cusp condition in all-electron calculations. The one-electron interaction term U_{en} describes the electron−nucleus correlation and satisfies the nuclear cusp condition. The U_{een} and U_{eenn} functions describe inhomogeneous two-electron interactions, which take into account the dynamical correlation effects between electrons, also improving the description of dispersive interactions.[45]

2.3. Computational Details. The Hartree−Fock (HF), DFT, complete active space (CASSCF), and n-electron valence state perturbation theory (NEVPT2) calculations have been done using the ORCA package.[46] For DFT we employed the 6-311G** basis set in accordance with ref 19, whereas for HF, CASSCF, and NEVPT2 we have used the cc-pVDZ basis set.

The structures of the conformers have been optimized at the DFT level using the B3LYP functional, in accordance with ref 19, in order to obtain results which were comparable with their high-level ab initio calculations, also done on the B3LYP/6-311G** optimized molecular structures.

The active space used for CASSCF and NEVPT2 includes all the relevant *d*-type orbitals involved in the Co coordination. In detail, for singlet and triplet structures (*a*, *c*, *d*, *f*, and *g*) an active space of eight electrons in eight molecular orbitals has been selected; for the doublet ones (*b* and *e*) nine electrons in eight orbitals have been used.

QMC calculations are carried out using the TurboRVB package[47] developed by Sorella and collaborators. The electronic structures of the cobalt-based molecular systems have been described through an unrestricted single Slater determinant wave function with the addition of a Jastrow factor, substituting the core electrons of the cobalt and oxygen atoms with energy-consistent pseudopotentials (ECP) with relativistic corrections.[48,49] The unrestricted Slater determinant is built from uncontracted Gaussian functions, whose exponents are taken from the Gaussian primitives of the ANO-VTZ basis set. Large exponents (i.e., > 50) have been removed due to the presence of ECPs, together with the *f* shells of the ANO-VTZ basis set.

Two basis sets for the U_{een} and U_{eenn} parts of the Jastrow factor (Table 1) have been defined using uncontracted Gaussian functions, in order to verify the convergence of our results with respect to the explicit Jastrow term. The first basis set is composed by Co(4s3p2d), O(3s2p1d), and H(2s1p) orbitals, whereas in the second one *f* orbitals are added for the cobalt.

Energy is minimized with respect to all the variational parameters, including the nonlinear Gaussian exponents of the Fermionic and many-body Jastrow expansion, using the method described in refs 43 and 50−52. The wave function optimization follows the computational procedure defined by some of us in previous works:[27,31,36,43] we start from previously optimized Slater-determinants at the DFT level with the ORCA package,[46] using B3LYP and PBE0 exchange-correlation functionals; afterwords, the Jastrow factor is added to the wave function, and its parameters are fully optimized at the VMC level while maintaining the orbital part frozen (the corresponding wave functions will be referred to as J-uB3LYP and J-uPBE0); after this step a full relaxation of all the parameters of the wave function, including the Gaussian primitives of the Fermionic basis set is taken on (the corresponding wave function will be referred to as J-uSD). For the LRDMC calculations a value of 0.04 bohr has been chosen for the space discretization step *a*, according to the analysis previously done in other works.[27,31,35]

Table 1. Jastrow Basis Set Convergence[c]

	reaction free energies (eV)	total energies (Hartree)	
basis set	a → b	a	b
*J*1[a]	2.42(2)	−247.3881(6)	−246.7012(4)
*J*2[b]	2.44(2)	−247.4114(4)	−246.7235(5)

[a]4s3p2d for Co, 3s2p1d for O, and 2s1p for H. All the QMC calculations have been performed using this basis set. [b]The same as *J*1 but with the addition of the *f* shell. [c]The J-uB3LYP wave function is used. Reaction free energies from a → b and total energies of a and b are listed here.

Zero-point energy (ZPE), thermal, enthalpy, and entropy corrections were taken into account in the computation of free-energy difference for each intermediate structure of the cycle. Normal-mode analysis was performed in order to get the ZPE correction, whereas the thermodynamic corrections were estimated at room temperature of 298.15 K and standard pressure of 1.00 atm. The ZPE corrections have been computed with different energy functionals with the 6-311G** basis set and are reported in Table S1 of the Supporting Information. Since the values of the corrections seem to be nearly identical for the different functionals, we have decided to apply corrections obtained with the B3LYP functional to all the free-energy values presented in this work, in accordance with ref 19. Rotational entropy of thermal corrections are evaluated assuming the complex to have C_1 point symmetry.

3. RESULTS AND DISCUSSION

The main goal of the present investigation is to quantitatively capture the interplay between electronic correlation and the energetics of the intermediate states along the water splitting reaction using a single-reference representation of the wave function.

For this reason the starting point of our analysis is the comparison of the free-energy profiles obtained with different DFT functionals, as shown in Figure 2. The total energies, the values of the $\langle S^2 \rangle$ operator, and the thermal corrections obtained for these calculations are reported in Table S1, while the energy and free-energy differences are collected in Table S2 of the Supporting Information. From Figure 2 we can see that the widely used hybrid functionals, such as B3LYP and PBE0, produce very similar free-energy profiles with a well distinguished maximum at step 5. Reducing the percentage of the exact HF exchange to 15%, as done for the B3LYP* functional,[53] has only the effect of giving a slightly smoother free-energy profile, still close to the B3LYP and PBE0 data.

DOI: 10.1021/acs.jctc.6b00632
J. Chem. Theory Comput. 2016, 12, 5803−5810

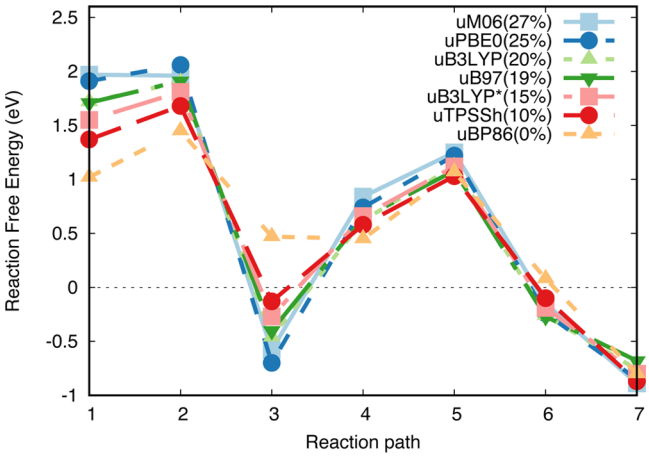

Figure 2. Reaction free-energy profile computed at the DFT level, using M06, PBE0, B3LYP, B97, B3LYP*, TPSSh, and BP86 functionals with the 6-311G** basis set.

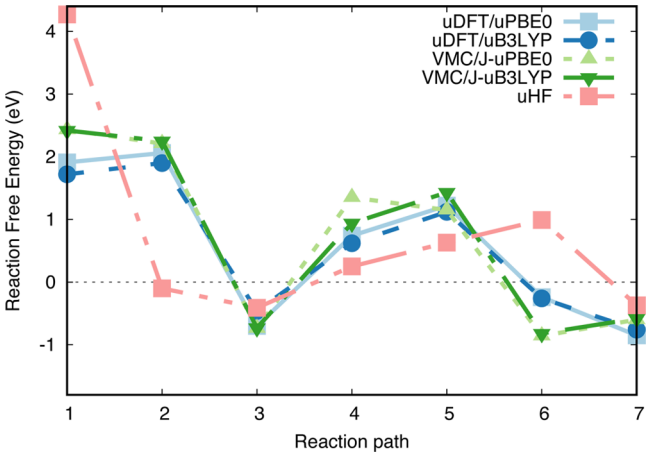

Figure 3. Reaction free-energy profile computed at the HF and DFT levels, using B3LYP and PBE0 functionals. VMC calculations with an optimized Jastrow term and B3LYP and PBE0 orbitals are also reported (J-uB3LYP and J-PBE0). Error bars for VMC are within the symbols.

Similar free-energy profiles are found for M06, B97, and TPSSh, while the GGA BP86 functional is characterized by the largest deviations with respect to the others. Also, the absolute value of the reaction free energies was increased as the percentage of the HF exchange increased.

Because of the overall compatibility of the DFT calculations with hybrid calculations, in order to construct the QMC starting wave functions we have decided to use the Kohn−Sham orbitals derived from the B3LYP and PBE0 calculations, also encouraged by the conclusions reported in ref 19 on the reliability of B3LYP and PBE0 for the electronic structure of cobalt complexes.

On this set of orbitals we have added and optimized the Jastrow factor, with the aim of understanding the role of the dynamical correlation introduced by this bosonic many-body term. In order to define a compact and still accurate Jastrow factor we have compared the performance of two different basis sets described in Section 2.3. In Table 1 we report the free-energy difference for the step $a \rightarrow b$, as a representative example of the full reaction path, and the corresponding total energies for a and b structures computed using the J-uB3LYP wave functions, with the $J1$ (without f functions) and with the $J2$ (with f functions) Jastrow terms. The Jastrow parameters are optimized minimizing the VMC energy, whereas the Slater determinant is kept fixed at the B3LYP molecular orbitals. As clearly expected, total energies with $J2$ are lower (about 0.02 hartree) than those with $J1$, but interestingly free-energy differences are equal within the statistical uncertainty implicit in the QMC approach. This important result allows us to use the smallest Jastrow factor for all the following QMC calculations presented in this work, considerably reducing the computational effort. Comparison among J-uB3LYP with the B3LYP functional, J-uPBE0 with the PBE0 functional, and HF is shown in Figure 3. The total energies are reported in Table 2, and the energy differences are reported in Table 3. HF is of course expected to give only a poor description of the electronic structure of the transition metal complex and, consequently, a bad estimation of the reaction free energy; thus, it is here taken only as a reference result in the absence of electronic correlation. At this level of theory (Figure 3) a large free-energy difference of 4.27 eV is found for removing one proton and one electron from the original complex (step 1), composed of three water molecules and three OH^- groups. Only a small minimum of less than −0.41 eV corresponds to step 3, i.e., the addition of one water molecule. The profile for the successive steps is completely different with respect to the DFT ones in Figure 2, with a maximum at step 6. The introduction of electronic correlation through DFT results in a more structured free-energy profile. As previously mentioned, hybrid B3LYP and PBE0 functionals give the same free-energy behavior along the reaction path: a first maximum at step 2 (1.90 and 2.06 eV, respectively), followed by the minimum at step 3 (−0.46 and −0.70 eV), and a further maximum at step 5 (1.12 and 1.22 eV).

The addition of the Jastrow factor to the unrestricted B3LYP and PBE0 wave functions, taking into explicit account the electron−electron distance, is seen to enhance the free-energy differences along the path, computed at the VMC level (Figure 3). In particular, the first maximum, on step 1 as for HF, is equal to 2.42(2) and 2.43(2) eV for the VMC/J-uB3LYP and VMC/J-uPBE0 treatments, whereas the second maximum (step 5) corresponds to 1.43(2) and 1.15(2) eV, respectively. The minimum at step 3 is the same (−0.73(3) vs −0.74(3) eV). The main difference between J-uB3LYP and J-uPBE0 is found for steps 4 and 5, i.e., the removal of one proton and one electron, otherwise the agreement is quantitative along the path, with the J-uB3LYP and J-uPBE0 VMC profiles practically identical within the error bars. VMC $\langle S^2 \rangle$ values for J-uB3LYP, J-uPBE0, and J-uSD are reported in Table S3.

LRDMC calculations fully recover the dynamical correlation, provided the nodal surface of the Slater determinant. The energy profiles obtained from these calculations are reported in Table 3 and displayed in Figure 4 together with the corresponding VMC results. Discrepancies in steps 4 and 5 between J-uB3LYP and J-uPBE0 are evidently reduced at the LRDMC level, whereas a reasonable agreement is maintained along the path, with differences at maximum of around 0.3 eV. Despite these small variations both the LRDMC results are essentially compatible within each other as also shown by the total energies in Table 2.

In order to get a full comprehension of the role of the specific choice of the molecular orbitals for the Fermionic part of the wave function, i.e. the Slater determinant, we have fully optimized the wave function at the VMC level of theory,

DOI: 10.1021/acs.jctc.6b00632
J. Chem. Theory Comput. 2016, 12, 5803−5810

Table 2. Total Energies (in Hartree) of the Different Structures for VMC and LRDMC Calculations

	VMC			LRDMC	
structure	J-uB3LYP	J-uPBE0	J-uSD	J-uB3LYP	J-uPBE0
a	−247.3881(6)	−247.3920(4)	−247.4219(2)	−247.608(2)	−247.612(2)
b	−246.7012(4)	−246.7041(4)	−246.7372(2)	−246.927(2)	−246.921(2)
c	−246.0217(9)	−246.0254(8)	−246.0615(2)	−246.249(2)	−246.245(2)
d	−263.3129(9)	−263.3183(8)	−263.3520(2)	−263.568(2)	−263.576(2)
e	−262.6786(5)	−262.6693(5)	−262.7150(2)	−262.932(2)	−262.934(2)
f	−262.0248(5)	−262.0257(5)	−262.0694(2)	−262.264(2)	−262.265(2)
g	−230.1051(5)	−230.1072(8)	−230.1378(2)	−230.299(2)	−230.299(2)

Table 3. Free Energies (in eV) for the Water Splitting Reaction at Different Levels of Theory

		uDFT		VMC			LRDMC	
step	HF	uB3LYP	uPBE0	J-uB3LYP	J-uPBE0	J-uSD	J-uB3LYP	J-uPBE0
1 a → b	4.27	1.72	1.91	2.42(2)	2.43(2)	2.29(1)	2.17(8)	2.45(8)
2 b → c	0.10	1.90	2.06	2.25(3)	2.21(2)	2.08(1)	2.13(8)	2.06(8)
3 c → d	−0.41	−0.46	−0.70	−0.73(3)	−0.74(3)	−0.56(1)	−0.88(8)	−1.19(8)
4 d → e	0.25	0.62	0.74	0.94(3)	1.35(2)	0.94(1)	0.90(8)	1.09(8)
5 e → f	0.63	1.12	1.22	1.43(2)	1.15(2)	1.14(1)	1.74(8)	1.77(8)
6 f → g	1.02	−0.26	−0.24	−0.82(2)	−0.86(2)	−0.69(1)	−0.55(8)	−0.52(8)
7 g → a	−0.37	−0.76	−0.85	−0.58(2)	−0.60(2)	−0.46(1)	−0.69(8)	−0.78(8)

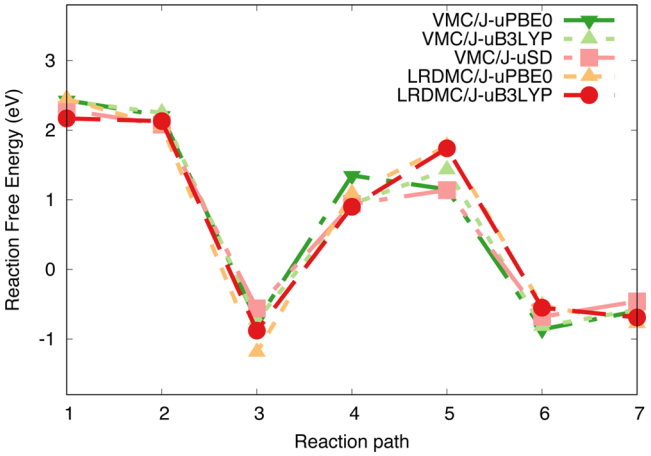

Figure 4. Comparison between the free-energy profiles obtained through the fully optimized VMC/J-uSD wave function and the VMC and LRDMC results given by the J-uB3LYP and J-uPBE0 wave functions obtained by adding the Jastrow factor to the molecular orbitals obtained through the B3LYP and PBE0 functionals. Error bars for VMC and LRDMC are within the symbols.

labeling the results as J-uSD. The total energies obtained are reported in Table 2, while the free energies are listed in Table 3. The reaction profile obtained with this optimized wave function is also compared in Figure 4 with the VMC and LRDMC, J-uB3LYP, and J-uPBE0 energy profiles.

By examining these results we can see that the free-energy profile obtained with the fully optimized J-uSD ansatz is only slightly changed with respect to the previous VMC and LRDMC calculations, with a small reduction (in absolute value) of energy differences when compared to the DFT-based values.

The full optimization of the wave function performed at the VMC level therefore does not dramatically affect the picture of the free energy with respect to the LRDMC and VMC results obtained with the J-uB3LYP and J-uPBE0 wave functions. A fundamental role in recovering the necessary electronic correlation is therefore played by the Jastrow factor more than by the specific choice of the molecular orbitals.

To check the quality of the ECPs used in QMC calculations, we have compared for DFT(B3LYP) calculations the full energy profile obtained by all-electron calculations (with different basis sets: 6-311G**, def2-TZVPP, ma-def2-TZVPP, ma-DKH-def2-TZVPP). The results show that the difference of reaction energies between the ECPs used in the present work[48,49] and the all-electron basis set def2-TZVPP were under 0.06 eV, confirming the reliability of ECPs used in this work (Table S4 and Figure S1).

Having verified the convergence of the QMC calculations, a comparison with the CCSD(T) data[19] is reported in Figure 5 and Table 4. Furthermore, in Table 4 we have added the total free-energy difference of the water oxidation process obtained with the VMC/J-uB3LYP, LRDMC/J-uB3LYP, and VMC/J-uSD and with the CCSD(T) method,[19] compared to the

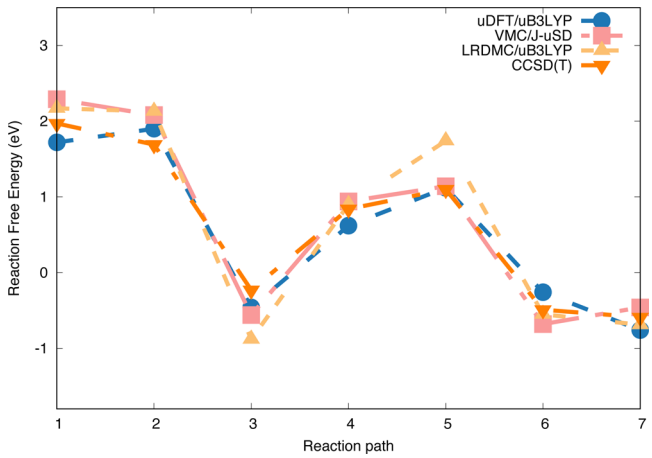

Figure 5. Comparison between the uDFT/B3LYP, J-uB3LYP/LRDMC, J-uSD/VMC, and CCSD(T)[19] free-energy profiles. Error bars for the VMC and LRDMC calculations are within the symbols.

DOI: 10.1021/acs.jctc.6b00632
J. Chem. Theory Comput. 2016, 12, 5803−5810

Table 4. Comparison between DFT (uB3LYP), QMC, CCSD(T),[19] and NEVPT2 Reaction Free Energies of the Water Splitting Reaction

step	VMC/J-uB3LYP	VMC/J-uSD	LRDMC/J-uB3LYP	uB3LYP	NEVPT2	CCSD(T)[19]	exp
1 a → b	2.42(2)	2.29(1)	2.17(8)	1.72	2.32	1.97	
2 b → c	2.25(3)	2.08(1)	2.13(8)	1.90	3.96	1.69	
3 c → d	−0.73(3)	−0.56(1)	−0.88(8)	−0.46	−2.29	−0.23	
4 d → e	0.94(3)	0.94(1)	0.90(8)	0.62	−0.04	0.84	
5 e → f	1.43(2)	1.14(1)	1.74(8)	1.12	1.96	1.10	
6 f → g	−0.80(2)	−0.69(1)	−0.55(8)	−0.26	−0.88	−0.49	
7 g → a	−0.58(2)	−0.46(1)	−0.69(8)	−0.76	−0.75	−0.59	
1 → 7	4.90(7)	4.75(3)	4.8(2)	3.89	4.28	4.29	4.92

experimental value of (1.23 × 4 = 4.92) eV in standard conditions and pH = 0.

We have to point out that at step 6 one O_2 molecule is formed in its triplet ground state, which turned out to be difficult to be described correctly due to strong dynamical correlation. In a previous investigation Zen et al.[34] demonstrated that QMC is able to quantitatively catch the electronic structure of the O_2 molecule; in particular LRDMC was seen to better perform with respect to CCSD(T) in describing the triplet-singlet gap. This consideration might eventually indicate that the CCSD(T) references may still be inadequate in fully recovering the correlation present in the O_2 ground state, explaining the differences with our free-energy profile. The LRDMC results presented here are based on the nodes of a single DFT determinant wave function. Whereas the overall behavior follows the VMC results, in step 5 LRDMC deviates from the other results, indicating that the DFT nodes might play an important role in describing this reaction step. A more detailed study of the dependence of the nodal surface on the DFT functional on that intermediate step might be the subject of future investigations.

Another clue of the quality of the QMC calculations can be found in the values of the water splitting free-energy. The QMC results (VMC/J-uSD, VMC/J-uB3LYP, and LRDMC/J-uB3LYP) are very close (or equal within the stochastic error implicit in the QMC formulation) to the experimental reference of 4.92 eV, whereas the CCSD(T) value (4.28 eV) is underestimated.

At last, since Kwapien et al.[19] suggested the possible role of the multiconfigurational nature of the structures appearing in the *c* and *f* steps in the catalytic process, we have investigated the role of static correlation by means of NEVPT2 calculations, based on the (8,8) active space for singlet and triplet states and (9,8) for the doublet ones. Unfortunately, by comparing the NEVPT2 results reported in Table 4 large differences appear between these multiconfigurational calculations and the QMC and CCSD(T) results. These large differences, also appearing between the configurations *c*, *d*, and *e* which were not recognized through the T_1 diagnostic[19] to be multiconfigurational, are probably due to the missing dynamical correlation of the CASSCF(8,8) starting guesses to which the perturbative correction is applied. This suggests that the differences observed between NEVPT2 and the single reference VMC/J-uSD, LRDMC/J-uB3LYP, and CCSD(T) are not strictly connected to the inclusion of excited configurations in the wave function. The largest discrepancies with respect to the single-reference approaches are found for steps 3 and 4, which share in common the structure *d*. The ground-state of this structure is substantially single-reference according to the CASSCF analysis, at least using the cc-pVDZ basis set. The same comment can be extended to the structure *e*, while the triplet *c* is correctly predicted as (partially) multiconfigurational. Also in the NEVPT2 case, the water splitting free energy is underestimated (4.29 eV).

Largest contributions from excited configurations to the ground-state wave function for the complexes along the reaction path (structures *b*, *c*, and *f*) are smaller than 20%.

The present results seem to support the idea that the most important ingredient for a correct description of the water splitting reaction catalyzed by the cobalt complex is the dynamic correlation, properly described by the Jastrow even in the presence of a single-reference wave function, whereas the static correlation only plays a minor role in the estimation of the free energies.

4. CONCLUSIONS

Artificial photosynthesis is an emerging research area in the field of energy research and materials science. Defining an efficient and cheap catalyst represents a fundamental task for both experimentalists and theoreticians. In this work we have computed the free-energy profile of the water splitting reaction, using a simplified computational model based on the cobalt ion, by means an efficient and accurate QMC procedure.

An unrestricted single-reference wave function multiplied by an optimized Jastrow factor has been employed, and calculations at VMC and LRDMC have been carried out. Since the most challenging task is the correct description of the dynamic electronic correlation, the use of a fully optimized Jastrow factor arises naturally as a powerful tool, at the expense of a single Slater determinant. We have verified that the inclusion of the Jastrow term in the wave function produces a VMC free-energy profile in fair agreement with the reference CCSD(T) coupled cluster calculations, even if the simple choice of using molecular orbitals from unrestricted B3LYP and PBE0 is done. The same general good agreement is found when the fully optimized J-uSD is used. The relaxation of the all the parameters, including the nonlinear exponents of the Gaussian function of the basis set expansion, leads to a variationally high-quality wave function, with the total energies, within the ECP scheme, well below the energies from J-uB3LYP and J-uPBE0. Moreover, the optimization of the determinant term makes the final results independent of the choice for the molecular orbitals. LRDMC calculations over the J-uB3LYP and J-uPBE0 wave functions confirm the free-energy profile already determined at the CCSD(T) level of theory.

The multiconfigurational analysis performed at the NEVPT2 level, including all the relevant orbitals for the correct description of the interaction between Co^{3+} and the various H_2O and OH^-, reveals small contributions of singly excited configurations for the triplet structures (as already pointed out

DOI: 10.1021/acs.jctc.6b00632
J. Chem. Theory Comput. 2016, 12, 5803−5810

by the CCSD(T) calculations) and for the doublet structure *b*. The NEVPT2 free-energy profile shows more pronounced maximum and minimum points, even though a qualitative analogy with the QMC results is conserved.

The definition of a compact but efficient wave function as J-uSD opens the way to the application of QMC to even larger multicenter transition metal complexes, overcoming the scaling issue intrinsic in the CCSD(T) method. The total free-energy differences for the water oxidation computed at the QMC level of theory are found in fair agreement with the experimental reference value, overperforming CCSD(T) and making us confident on the highly accurate results obtained by the present computational approach.

■ ASSOCIATED CONTENT

Supporting Information

The Supporting Information is available free of charge on the ACS Publications website at DOI: 10.1021/acs.jctc.6b00632.

Table S1, total energies, thermal corrections, and $\langle \hat{S}^2 \rangle$ values of the seven structures of the water splitting reaction proposed here with the different DFT functionals; Table S2, reaction and reaction free energies of the catalytic reaction with the cobalt water complex computed by different DFT functionals; Table S3 $\langle \hat{S}^2 \rangle$ for VMC calculations; Table S4 and Figure S1, comparison between ECP and all-electron results for the B3LYP reaction energies (PDF)

■ AUTHOR INFORMATION

Corresponding Author

*E-mail: leonardo.guidoni@univaq.it.

Notes

The authors declare no competing financial interest.

■ ACKNOWLEDGMENTS

The authors acknowledge the CINECA supercomputing centre, the PRACE infrastructure, and the Caliban supercomputing centre of the University of L'Aquila for computational support. E.C. thanks Eleonora Luppi and Julien Toulouse for support.

■ REFERENCES

(1) Lewis, N. S.; Nocera, D. G. *Proc. Natl. Acad. Sci. U. S. A.* **2006**, *103*, 15729−15735.
(2) Barber, J. *Chem. Soc. Rev.* **2009**, *38*, 185−196.
(3) Cook, T. R.; Dogutan, D. K.; Reece, S. Y.; Surendranath, Y.; Teets, T. S.; Nocera, D. G. *Chem. Rev.* **2010**, *110*, 6474−6502.
(4) Nocera, D. G. *Acc. Chem. Res.* **2012**, *45*, 767−776.
(5) Artero, V.; Chavarot-Kerlidou, M.; Fontecave, M. *Angew. Chem., Int. Ed.* **2011**, *50*, 7238−7266.
(6) Gust, D.; Moore, T. A.; Moore, A. L. *Faraday Discuss.* **2012**, *155*, 9−26.
(7) Sartorel, A.; Bonchio, M.; Campagna, S.; Scandola, F. Tetrametallic molecular catalysts for photochemical water oxidation. *Chem. Soc. Rev.* **2013**, *42*, 2262−2280.
(8) Mattioli, G.; Giannozzi, P.; Bonapasta, A. A.; Guidoni, L. *J. Am. Chem. Soc.* **2013**, *135*, 15353−15363.
(9) Kärkäs, M. D.; Verho, O.; Johnston, E. V.; Åkermark, B. *Chem. Rev.* **2014**, *114*, 11863−12001.
(10) Blakemore, J. D.; Crabtree, R. H.; Brudvig, G. W. *Chem. Rev.* **2015**, *115*, 12974−13005.
(11) Schilling, M.; Patzke, G. R.; Hutter, J.; Luber, S. *J. Phys. Chem. C* **2016**, *120*, 7966−7975.
(12) Retegan, M.; Krewald, V.; Mamedov, F.; Neese, F.; Lubitz, W.; Cox, N.; Pantazis, D. A. *Chem. Sci.* **2016**, *7*, 72−84.
(13) Kanan, M. W.; Nocera, D. G. *Science* **2008**, *321*, 1072−1075.
(14) La Ganga, G.; Puntoriero, F.; Campagna, S.; Bazzan, I.; Berardi, S.; Bonchio, M.; Sartorel, A.; Natali, M.; Scandola, F. *Faraday Discuss.* **2012**, *155*, 177−190.
(15) Evangelisti, F.; Güttinger, R.; Moré, R.; Luber, S.; Patzke, G. R. *J. Am. Chem. Soc.* **2013**, *135*, 18734−18737.
(16) Mattioli, G.; Risch, M.; Bonapasta, A. A.; Dau, H.; Guidoni, L. *Phys. Chem. Chem. Phys.* **2011**, *13*, 15437−15441.
(17) Mattioli, G.; Zaharieva, I.; Dau, H.; Guidoni, L. *J. Am. Chem. Soc.* **2015**, *137*, 10254−10267. 00009.
(18) Wang, L.-P.; Van Voorhis, T. *J. Phys. Chem. Lett.* **2011**, *2*, 2200−2204.
(19) Kwapien, K.; Piccinin, S.; Fabris, S. *J. Phys. Chem. Lett.* **2013**, *4*, 4223−4230.
(20) Nørskov, J. K.; Rossmeisl, J.; Logadottir, A.; Lindqvist, L.; Kitchin, J. R.; Bligaard, T.; Jónsson, H. *J. Phys. Chem. B* **2004**, *108*, 17886−17892.
(21) Foulkes, W. M. C.; Mitas, L.; Needs, R. J.; Rajagopal, G. *Rev. Mod. Phys.* **2001**, *73*, 33−83.
(22) Scemama, A.; Caffarel, M.; Oseret, E.; Jalby, W. *J. Comput. Chem.* **2013**, *34*, 938−951.
(23) Barborini, M.; Guidoni, L. *J. Chem. Theory Comput.* **2015**, *11*, 4109−4118.
(24) Coccia, E.; Varsano, D.; Guidoni, L. *J. Chem. Theory Comput.* **2013**, *9*, 8−12.
(25) Coccia, E.; Varsano, D.; Guidoni, L. *J. Chem. Theory Comput.* **2014**, *10*, 501−506.
(26) Zen, A.; Luo, Y.; Mazzola, G.; Guidoni, L.; Sorella, S. *J. Chem. Phys.* **2015**, *142*, 144111.
(27) Zen, A.; Coccia, E.; Luo, Y.; Sorella, S.; Guidoni, L. *J. Chem. Theory Comput.* **2014**, *10*, 1048−1061.
(28) Austin, B. M.; Zubarev, D. Y.; Lester, W. A. *Chem. Rev.* **2012**, *112*, 263−288.
(29) Coccia, E.; Guidoni, L. *J. Comput. Chem.* **2012**, *33*, 2332−2339.
(30) Barborini, M.; Sorella, S.; Guidoni, L. *J. Chem. Theory Comput.* **2012**, *8*, 1260−1269.
(31) Coccia, E.; Chernomor, O.; Barborini, M.; Sorella, S.; Guidoni, L. *J. Chem. Theory Comput.* **2012**, *8*, 1952−1962.
(32) Zen, A.; Luo, Y.; Sorella, S.; Guidoni, L. *J. Chem. Theory Comput.* **2013**, *9*, 4332−4350.
(33) Varsano, D.; Coccia, E.; Pulci, O.; Conte, A. M.; Guidoni, L. *Comput. Theor. Chem.* **2014**, *1040-1041*, 338−346.
(34) Zen, A.; Trout, B. L.; Guidoni, L. *J. Chem. Phys.* **2014**, *141*, 014305.
(35) Zen, A.; Coccia, E.; Gozem, S.; Olivucci, M.; Guidoni, L. *J. Chem. Theory Comput.* **2015**, *11*, 992−1005.
(36) Barborini, M.; Coccia, E. *J. Chem. Theory Comput.* **2015**, *11*, 5696−5704.
(37) Barborini, M.; Guidoni, L. *J. Chem. Theory Comput.* **2015**, *11*, 508−517.
(38) Doblhoff-Dier, K.; Meyer, J.; Hoggan, P. E.; Kroes, G.-J.; Wagner, L. K. *J. Chem. Theory Comput.* **2016**, *12*, 2583−2597.
(39) Bressanini, D.; Reynolds, P. J. *Advances in Chemical Physics, Monte Carlo Methods in Chemical Physics*; 1998; Vol. *105*, pp 5345−5350.
(40) Reynolds, P. J.; Ceperley, D. M.; Alder, B. J.; Lester, W. A. *J. Chem. Phys.* **1982**, *77*, 5593.
(41) Casula, M.; Filippi, C.; Sorella, S. *Phys. Rev. Lett.* **2005**, *95*, 100201.
(42) Casula, M.; Moroni, S.; Sorella, S.; Filippi, C. *J. Chem. Phys.* **2010**, *132*, 154113.
(43) Marchi, M.; Azadi, S.; Casula, C.; Sorella, S. *J. Chem. Phys.* **2009**, *131*, 154116.
(44) Drummond, N. D.; Towler, M. D.; Needs, R. J. *Phys. Rev. B: Condens. Matter Mater. Phys.* **2004**, *70*, 234119.
(45) Sterpone, F.; Spanu, L.; Ferraro, L.; Sorella, S.; Guidoni, L. *J. Chem. Theory Comput.* **2008**, *4*, 1428−1434.
(46) Neese, F. *WIREs Comput. Mol. Sci.* **2012**, *2*, 73−78.

DOI: 10.1021/acs.jctc.6b00632
J. Chem. Theory Comput. 2016, 12, 5803−5810

(47) Sorella, S. *TurboRVB* Quantum Monte Carlo package. http://people.sissa.it/~sorella/web/index.html (accessed Feb 2016).
(48) Burkatzki, M.; Filippi, C.; Dolg, M. *J. Chem. Phys.* **2007**, *126*, 234105.
(49) Burkatzki, M.; Filippi, C.; Dolg, M. *J. Chem. Phys.* **2008**, *129*, 164115.
(50) Toulouse, J.; Umrigar, C. J. *J. Chem. Phys.* **2007**, *126*, 084102.
(51) Umrigar, C. J.; Toulouse, J.; Filippi, C.; Sorella, S.; Hennig, R. G. *Phys. Rev. Lett.* **2007**, *98*, 110201.
(52) Toulouse, J.; Umrigar, C. J. *J. Chem. Phys.* **2008**, *128*, 174101.
(53) Reiher, M.; Salomon, O.; Hess, B. A. *Theor. Chem. Acc.* **2001**, *107*, 48−55.

DOI: 10.1021/acs.jctc.6b00632
J. Chem. Theory Comput. 2016, 12, 5803−5810